Enhancement of UV disinfection of urine matrixes by electrochemical oxidation

Miguel Herraiz-Carboné[1], Salvador Cotillas[1*], Engracia Lacasa[1], Pablo Cañizares[2], Manuel A. Rodrigo[2], Cristina Sáez[2*]

[1] Department of Chemical Engineering, Higher Technical School of Industrial Engineering, University of Castilla-La Mancha, Edificio Infante Don Juan Manuel, Campus Universitario s/n, 02071 Albacete, Spain

[2] Department of Chemical Engineering, Faculty of Chemical Sciences and Technologies, University of Castilla-La Mancha, Edificio Enrique Costa Novella, Campus Universitario s/n, 13005 Ciudad Real, Spain

Abstract

This work focuses on the removal of antibiotic-resistant bacteria (ARB) contained in hospital urines by UV disinfection enhanced by electrochemical oxidation to overcome the limitations of both single processes in the disinfection of this type of effluents. UV disinfection, electrolysis, and photoelectrolysis of synthetic hospital urine intensified with *K. pneumoniae* were studied. The influence of the current density and the anode material was assessed on the disinfection performance of combined processes and the resulting synergies and/or antagonisms of coupling both technologies were also evaluated. Results show that the population of bacteria contained in hospital urine is only reduced by 3 orders of magnitude during UV disinfection. Electrolysis leads to complete disinfection of hospital urine when working at 50 A m^{-2} using Boron Doped Diamond (BDD) and Mixed Metal Oxides (MMO) as anodes. The coupling of electrolysis to the UV disinfection process leads to the highest disinfection rates, attaining a complete removal of ARB for all the current densities and anode materials tested. The use of MMO anodes leads to higher synergies than BDD electrodes. Results confirm that UV disinfection can be enhanced by electrolysis for the removal of ARB in urine, considering both technical and economic aspects.

Keywords

UV disinfection; electrolysis; photoelectrolysis; antibiotic-resistant bacteria; urine

Highlights

- UV disinfection decreases *K. pneumoniae* in hospital urine by 3-logs.
- Electrolysis ensures a complete bacteria removal with BDD and MMO anodes at 50 Am^{-2}.
- The highest disinfection rates are obtained during photoelectrolysis.
- Synergies are found when coupling UV disinfection and electrolysis at 5 A m^{-2}.
- Hypochlorite and chloramines are the main responsible species for disinfection.

*authors to whom all correspondence should be addressed (corresponding authors): cristina.saez@uclm.es; salvador.cotillas@uclm.es . Tel.: +34-926-29-53-00 Ext. 6708

1. Introduction

In last years, concern about hospital wastewater treatment has sharply increased in the scientific community, not only related to the presence of a great variety of drugs but also for the high concentration of pathogens, viruses, and fungi [1, 2]. Wastewater generated in hospital facilities may have very different sources (laundry, kitchen, toilets…) and among them, hospital urine can be considered as the main hotspot of both drugs and microorganisms, despite urine only constitutes 2-3 % of the total volume of wastewater generated [3]. In turn, hospital wastewater (including urine) is merged with urban wastewater and treated in conventional wastewater treatment plants (WWTPs) that are not able to efficiently remove the microorganisms owing to the limitations of the technology used [4, 5]. This promotes the occurrence of antibiotic-resistant bacteria (ARB) [6, 7], one of the biggest threats of global health, food security, and development today considered by the World Health Organization (WHO). To prevent the appearance of ARB, hospital urines could be pre-treated before its merge with hospital wastewater and the subsequent discharge to WWTP, using advanced and efficient processes for the removal of microorganisms.

To the authors´ knowledge, the disinfection of urine has not been studied in-depth and few recent works have been previously reported in the literature [8-10]. Researches focused on the disinfection of urban and hospital wastewater have been more regular, using different Advanced Oxidation Processes (AOPs) among other techniques [11-13]. One of the AOPs widely evaluated for the treatment of urban and hospital wastewater is ultraviolet (UV) disinfection [13-15]. The irradiation of UV light to an effluent containing microorganisms can promote bacteria removal by destroying the genetic material [16]. Likewise, UV light can penetrate the cell wall, destroying the genetic material. However, the damage caused on bacteria can be repaired after relatively small times, promoting

bacteria regrowth [17, 18]. Besides, the presence of suspended solids and colloids in wastewater decreases the process efficiency. This can be an important drawback in the removal of ARB in hospital urines and this should be taken into consideration to ensure efficient and persistent disinfection.

At this point, the use of combined treatments appears as a good option to overcome these limitations. Among the different alternatives, electrochemical oxidation is a potential candidate to be considered. Depending on the electrode material and applied current density [19, 20], this technology can promote the formation of hydroxyl radicals from water electrolysis and has been satisfactorily tested for the disinfection of urban wastewater and even hospital urines [9, 21, 22]. Furthermore, during electrolysis, other oxidants can be generated from the oxidation of the ions naturally contained in the effluents that can also contribute to the disinfection process, preventing the bacteria regrowth. At this point, the role of anode material is critical. Thus, the use of anodes based on Mixed Metal Oxides (MMO) such as RuO_2, IrO_2, or Ta_2O_5 promotes the evolution of chlorine during electrolysis [23-25]. On the other hand, Boron Doped Diamond (BDD) anodes favour the formation of a cocktail of oxidants (e.g., hypochlorite, persulfate, peroxodiphosphate, percarbonate, ozone) which seems to be the main responsible for the good performance of this electrode in the treatment of industrial wastewater [26, 27] and wastewater disinfection [28, 29].

With this background, the goal of this work is to evaluate the synergies or antagonisms when coupling electrochemical oxidation to UV disinfection for the removal of ARB in hospital urines. To do this, *Klebsiella pneumoniae* (*K. pneumoniae*) has been selected as a model of ARB because it is mainly excreted in urine [30, 31]. It is a gram-negative bacteria that belongs to the Enterobacteriaceae family and presents antibiotic resistance to third-generation cephalosporins and carbapenems [32, 33]. UV disinfection,

104 electrolysis, and the combined process (photoelectrolysis) were carried out using an
105 electrochemical microfluidic flow-through reactor, paying special attention to the
106 influence of the current density (5-50 A m^{-2}) and the anode material (BDD and MMO).
107 This will allow us to assess if the UV disinfection process can be enhanced for the
108 removal of ARB in very complex media such as from hospital urines.
109

110 **2. Material and methods**

111 **2.1. Chemicals and microorganisms**

112 Compounds employed for the formulation of synthetic urine (urea, creatinine, uric
113 acid, potassium chloride, magnesium sulfate, calcium phosphate, sodium carbonate, and
114 diammonium hydrogen phosphate) were analytical grade and used as received (Sigma
115 Aldrich, Spain). The bacterial strain used during UV disinfection, electrolysis, and
116 photoelectrolysis was *K. pneumoniae* ATCC 4352 (CECT, Spain). Potassium phosphate
117 monobasic, sodium phosphate dibasic, ethylenediaminetetraacetic acid (EDTA), N,N-
118 Diethyl-p-phenylenediamine sulfate (Sigma Aldrich, Spain), and sulfuric acid (VWR)
119 were used for the determination of chloramines. Acetone, 2,6-pyridinedicarboxylic acid,
120 and nitric acid (Sigma Aldrich, Spain) were used for the determination of ion
121 concentrations. Arsenic trioxide used for the determination of hypochlorite ion was also
122 purchased by Sigma Aldrich, Spain. All chemicals used for analytical measurements were
123 analytical grade and used as received. Double deionized water (Millipore Milli-Q system,
124 resistivity: 18.2 MΩ cm at 25 °C) was used to prepare all solutions.
125

126

2.2. Experimental procedure

UV disinfection process was carried out in a cylindrical reactor made of borosilicate where a UV germicidal lamp of 5 W ($\lambda = 254$ nm) was located in the middle of the system. Infected synthetic urine (2 dm^3) was recirculated with a peristaltic pump (Percom N-M, JP Selecta) to favor the mass transfer in the photoreactor. Electrolysis experiments were developed in a microfluidic flow-through electrochemical cell equipped with mesh electrodes. Boron Doped Diamond (BDD) and Mixed Metal Oxides (MMO) were used as anodes and Stainless Steel (SS) as the cathode. BDD anode consisted of a thin diamond film supported on a niobium mesh (Diachem®) with a size of 9.5×8 cm^2, supplied by Condias GmbH (Germany). MMO anode consisted of an IrO_2/Ta_2O_5 (70:30) coated titanium mesh with a total dimension of 9.5×8 cm^2, supplied by Tianode (India). The surface area was 53 and 50 cm^2 for MMO and BDD, respectively [34]. A Delta Electronika ES030-10 power supply (0-30V, 0-10A) provided the electric current. The effluent was recirculated with a peristaltic pump. Photoelectrolysis was carried out by coupling the photoreactor used for the UV disinfection process to the microfluidic flow-through electrochemical reactor. A detail of the experimental setup used is shown in Fig. S1. All electrochemical and photoelectrochemical experiments were employed under galvanostatic conditions with an initial volume of 2 dm^3 and a flow rate of 40 $dm^3\ h^{-1}$. Current densities applied were between 5 and 50 A m^{-2}. These values have been selected considering the two different limit behaviors of electrolysis: direct oxidation which is promoted at low current densities (5 A m^{-2}) and mediated oxidation that is expected to prevail when working at 50 A m^{-2} [35, 36]. All experiments were conducted in triplicate.

The simulated hospital urine was prepared with synthetic human urine as supporting electrolyte intensified with *K. pneumoniae* (10^6 CFU mL^{-1}). Table 1 shows the composition of the synthetic urine used in this work [37].

Table 1. Composition of the synthetic urine.

Compound	Concentration (mg dm^{-3})
CH_4N_2O	3333.34
$C_4H_7N_3O$	166.67
$C_5H_4N_4O_3$	50.00
KCl	1000.00
$MgSO_4$	170.00
$(Ca)_3(PO_4)_2$	28.34
Na_2CO_3	166.67
$(NH_4)_2HPO_4$	83.34

2.3. Analytical methods

Bacteria (*K. pneumoniae*) counts were performed by an indirect impedance method using a μ-Trac® 4200 system. It uses a standard impedance signal (Media Impedance = M-value) that is registered as the result of microbial metabolism, which causes the change of the impedance in an AC field. During the growth of microorganisms low or non-charged nutrient molecules are metabolized. This break down of nutrients generates small and highly charged metabolites that result in a change of the impedance of the nutrient media that is recorded by the instrument [38, 39]. The impedance values are related to the concentration of *K. pneumoniae* in CFU mL^{-1} through an initial calibration of the equipment by plate counts.

The DPD (N,N-diethyl-phenylenediamine) standard colorimetric method [40], was used for the determination of inorganic chloramines. This is a selective method that allows us to determine the presence of mono-, di- and trichloramine without the interferences of

other oxidizing species formed during the process, such as, ozone or hydrogen peroxide. Ion chromatography (IC), Metrohm 930 Compact IC Flex coupled to a conductivity detector, was used to analyze the inorganic ions. The columns Metrosep A Supp 7 and Metrosep C6 250 were used to measure anions and cations, respectively. The mobile phase of 85:15 v/v 3.6 mM Na_2CO_3/acetone with a flow rate of 0.8 cm^3 min^{-1} was used to measure anions and a mobile phase of 1.7 mM HNO_3 + 1.7 mM 2,6-pyridinedicarboxylic acid with a flow rate of 0.9 cm^3 min^{-1} was employed for cations. The volume injection of each sample was 20 µL. The peak of the chromatogram for hypochlorite interferes with the chloride peak in the IC technique, therefore, hypochlorite was analyzed by titration with 0.001 M As_2O_3 in 2 M NaOH [41, 42]. This analytical technique is selective in measuring anion hypochlorite. The pH and conductivity were simultaneously measured using a Sension+ MM150 Portable Multi-Parameter Meter from HACH.

3. Results and discussion

Fig. 1 shows changes in the concentration of *K. pneumoniae* with the operation time during the UV disinfection, electrodisinfection, and photo-electrodisinfection of hospital urines. As can be observed, UV disinfection reduces 3 orders of magnitude the concentration of bacteria in hospital urine after 3 hours of treatment. The removal of microorganisms may be due to the penetration of UV light into the cell, destroying the genetic material [43]. Two zones can be distinguished in which the disinfection rate is very different. Initially, the inactivation of *K. pneumoniae* is very fast, reaching the maximum log removal around 30 min (zone I). After that, the disinfection rate decreases drastically (zone II). This behavior has also been reported in the literature during the

application of the UV disinfection process to the treatment of wastewater, although the occurrence of a plateau zone has not yet been clearly explained [44, 45]. Several hypotheses have been proposed such as the aggregation of microorganisms or a resistant subpopulation, but no clear evidences have been reported [17].

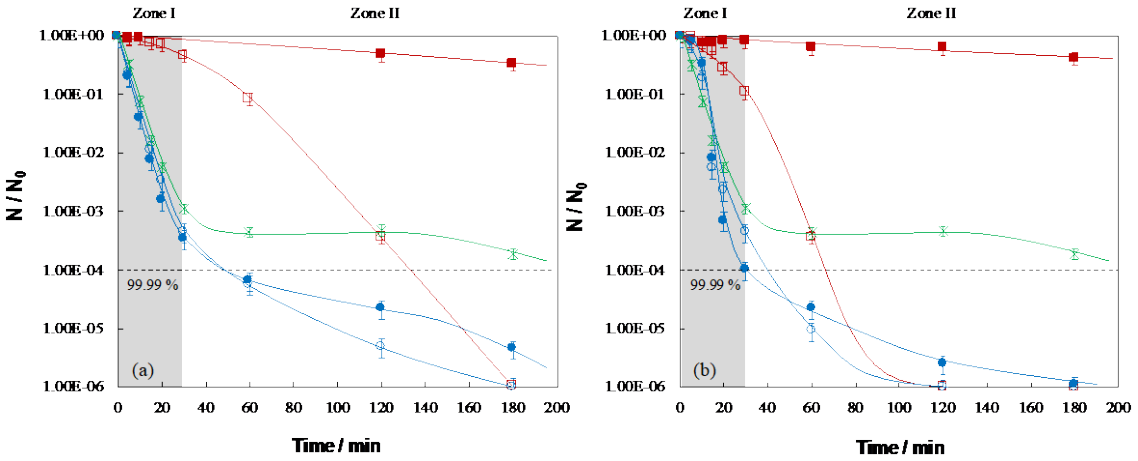

Fig. 1. Time course of the concentration of *K. pneumoniae* during the treatment of hospital urines. Green symbols (x): UV disinfection; red symbols (■, □): electrolysis; blue symbols (●, ○): photoelectrolysis; full symbols: 5 A m^{-2}; empty symbols: 50 A m^{-2}; (a) BDD anode; (b) MMO anode. *K. pneumoniae*$_0$ (N_0): 10^6 CFU mL^{-1}.

On the other hand, complete inactivation of *K. pneumoniae* can be attained in hospital urines using electrolysis with BDD and MMO anodes at 50 A m^{-2}, while at low current densities (5 A m^{-2}) the population of microorganisms slightly decreases without removing 1 order of magnitude, regardless the anode material used. This reveals that a minimum current density (higher than 5 A m^{-2}) should be applied to ensure complete disinfection. However, different trends can be seen during electrolysis at higher current densities with both anodes. Specifically, an operation time of 180 min (which corresponds with 0.42 Ah dm^{-3} of electric charge) is needed for killing bacteria with BDD anodes whereas a total inactivation is achieved in 120 min (which corresponds with 0.28 Ah dm^{-3} of electric

charge) using MMO electrodes at 50 A m^{-2}. This is an unexpected behavior because electrochemical disinfection with BDD is generally more efficient and faster than with MMO anodes [46]. Nonetheless, it should be noted that the properties of diamond anodes significantly influence the performance of an electrochemical process [47-49] and therefore, general conclusions should not be drawn for all diamond electrodes. The electrode used in the work was made over a niobium substrate, which has shown not to promote the production of large amounts of powerful oxidants during electrolysis, as tantalum and silicon substrates [50]. So, this could explain the lower disinfection rate registered in comparison with MMO anodes. Likewise, it is important to point out that the MMO anodes used are based on IrO_2/Ta_2O_5 which favors the evolution of oxygen and chlorine during electrolysis and the subsequent disinfection process [51]. A detailed discussion related to the influence of the anode material on the production of oxidants during electrochemical disinfection is reported later. Nevertheless, at this point, it should be mentioned that the concentration of *K. pneumoniae* was also measured after 24 h to evaluate a possible bacteria regrowth. For this additional test, samples were stored in dark at room temperature when finishing the experiments. The population of microorganisms was similar to that obtained at the end of electrolysis which confirms that the electrochemical process ensures persistent disinfection.

Regarding the photoelectrolysis process, results obtained show the highest disinfection rates, reaching a reduction higher than 5 orders of magnitude for all the current densities and anode materials tested. The removal of *K. pneumoniae* follows the same profile as UV disinfection at the beginning of the treatment (Zone I), reaching 3-4 orders of magnitude reduction for both anodes, regardless the current density applied. Then, unlike behavior observed during single photolysis, the population of microorganisms continuous to decrease until the total disinfection (Zone II), being the removal rate higher at 50 A m^{-}

234 ^{2}. Photoelectrolysis is much better than single processes since improves 2-3 orders of
235 magnitude the UV disinfection process and even 5-6 orders of magnitude the
236 electrochemical process at 5 A m^{-2}. At high current densities, electrochemical and
237 photoelectrochemical processes attain complete disinfection but the last one shows a
238 higher removal rate. Likewise, the use of MMO anodes leads to higher disinfection rates
239 in comparison with BDD anodes due to their different electrocatalytic properties for the
240 production of disinfectants [52]. In this context, the large amounts of disinfectants
241 generated during the electrolysis of hospital urines [9] can be activated by the irradiation
242 of UV light, favoring the production of free radicals which are more reactive than the
243 parent oxidants [53]. Hence, the higher disinfection efficiency can be attributed to the
244 photo-activation of oxidants during the combined treatment. The two different zones
245 observed indicate that the contribution of UV light irradiation is more significant at the
246 beginning of the process (zone I) whereas the combination of photochemical and
247 electrochemical processes leads to remarkable synergies in the disinfection at the end of
248 the treatment (zone II). Likewise, the low electric charges applied within 30 min of the
249 experiments ($Q < 0.1$ Ah dm^{-3}) may support the almost negligible contribution of
250 electrochemical oxidation at the beginning of the treatment because of the expected low
251 generation and accumulation of disinfectants in the system.

252 For comparison purposes, experimental data were fitted to a first-order kinetic model and,
253 the resulting kinetic constants, the residual variance (S^2_R), and the correlation coefficient
254 (R^2) are presented in Table 2. Two different values have been calculated for
255 photochemical and photoelectrochemical processes that correspond to the different zones
256 observed in the removal of microorganisms and only one value is reported for the single
257 electrochemical process.

Comparing the combined process with UV disinfection, the kinetic constants are a little higher in the zone I during photoelectrolysis, which confirms that there exists a small contribution of the electrochemical process to the removal of microorganisms at the beginning of the treatment. On the contrary, the values registered in zone II are much higher, being more noticeable at higher current densities where the production of oxidants is expected to be higher by electrolysis and, hence, the disinfection rate. These results point out the higher contribution of the electrochemical process at the end of the treatment. To quantify the improvement of UV disinfection by electrolysis, the synergy coefficient was calculated according to Eq. 1 [54]. Fig. 2 shows the synergy coefficient for the combined process and the logarithmic removal increase between UV disinfection and photoelectrolysis.

Table 2. Kinetic constants for the disinfection by UV irradiation, electrolysis, and photoelectrolysis.

Process	**Anode material**	**Current density ($A\ m^{-2}$)**	$k_{Zone\ I}$ **(min^{-1})**	S^2_R **(CFU^2/mL^2)**	R^2	$k_{Zone\ II}$ **(min^{-1})**	S^2_R **(CFU^2/mL^2)**	R^2
UV disinfection	-	-	0.2338	0.1327	0.9795	0.0098	0.1498	0.7141
Electrolysis*	BDD	5	0.0062	0.0002	0.9992	0.0062	0.0002	0.9992
		50	0.0770	0.5861	0.9747	0.0770	0.5861	0.9747
	MMO	5	0.0039	0.0125	0.8193	0.0039	0.0125	0.8193
		50	0.1400	0.4833	0.9848	0.1400	0.4833	0.9848
Photoelectrolysis	BDD	5	0.3247	0.0003	0.9999	0.0269	0.1967	0.9411
		50	0.2570	0.1237	0.9842	0.0428	0.2258	0.9726
	MMO	5	0.3491	1.2676	0.9168	0.0301	0.3666	0.9135
		50	0.2926	0.9813	0.9089	0.062	2.2737	0.7498

*only one zone

$$\text{Synergy coefficient} = \frac{k_{photoelectrolysis}}{k_{UV\ disinfection} + k_{electrolysis}} \quad (1)$$

A synergistic effect resulted in the disinfection of urines during photoelectrolysis at 5 A m^{-2}, regardless the anode material used. Under these conditions, there is a marked contribution of UV disinfection at the beginning of the treatment and then, the electrochemical process has a more significant influence on the removal of ARB. The highest synergistic effect was obtained in zone II during photoelectrolysis with MMO anodes where the disinfection by UV irradiation is very limited. These synergies could be explained by the generation and photoactivation of the disinfectant species formed during the combined process. More details about the disinfectants produced during the different processes tested are reported later. At higher current densities, antagonistic effects (synergy coefficient < 1) can be observed during photoelectrolysis with both anodes. This can be due to the competitive oxidation between *K. pneumoniae* and organics contained in the urine matrix (urea, creatinine, and uric acid) under these operating conditions [55]. These results reveal that photoelectrolysis is an efficient technology for the disinfection of hospital urines when working at low current densities since electrolysis can enhance by 2 orders of magnitude the removal of *K. pneumoniae* attained by UV disinfection. The use of current densities of 50 A m^{-2} improves the removal in 3 orders of magnitude but clear antagonistic effects have been obtained.

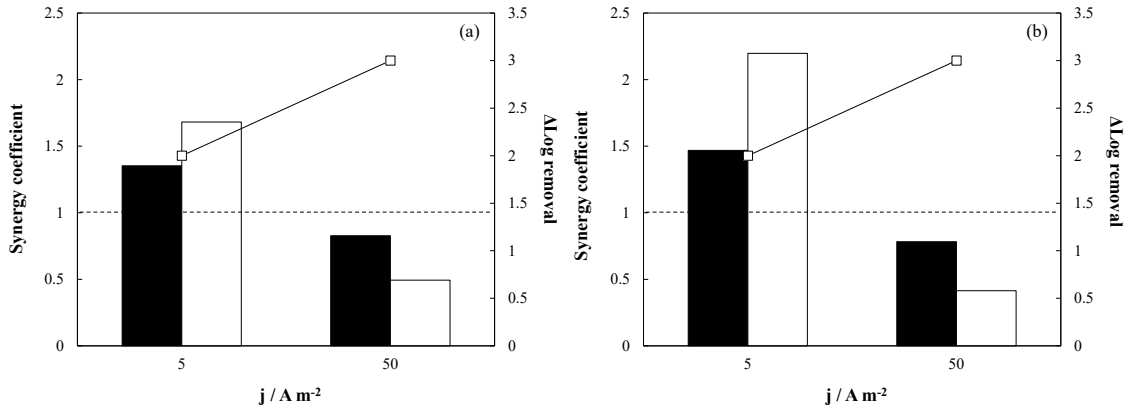

Fig. 2. Synergistic effect (bars) and ΔLog removal (points) calculated at different current densities. Black bars: zone I; white bars: zone II; (a) BDD anode; (b) MMO anode.

The removal of ARB from urine by electrochemical processes could take place by the direct oxidation of microorganisms over the anode surface (electroadsorption) or by mediated oxidation via electrogenerated oxidants. The first option mainly occurs when using porous materials such as carbon felt or cloth as the anode, where bacteria can be adsorbed [56]. On the other hand, the in-situ production of disinfectants and the subsequent attack to microorganisms seems to be the main mechanism for killing bacteria during electrolysis with BDD and MMO anodes [9, 57]. Urine matrix used in this work contains large amounts of chloride in its composition (475.52 mg dm^{-3}) whose first oxidation product is hypochlorite (Eqs. 2-4).

$$2\ Cl^- \rightarrow Cl_{2(aq)} + 2\ e^- \quad (E^0 = -1.36\ V) \tag{2}$$

$$Cl_{2(aq)} + H_2O \rightarrow HClO + Cl^- + H^+ \quad (E^0 = -1.63\ V) \tag{3}$$

$$HClO \rightleftharpoons H^+ + ClO^- \tag{4}$$

This species is a well-known disinfectant that is used in conventional disinfection processes [58] and, for this reason, its concentration was monitored during the treatment. Fig. 3 shows the hypochlorite electrogenerated as a function of the operation time during the disinfection of hospital urines by electrolysis and photoelectrolysis with BDD and MMO anodes at the current densities tested. Data from UV disinfection is not included in the figure because hypochlorite was not detected during this photochemical process.

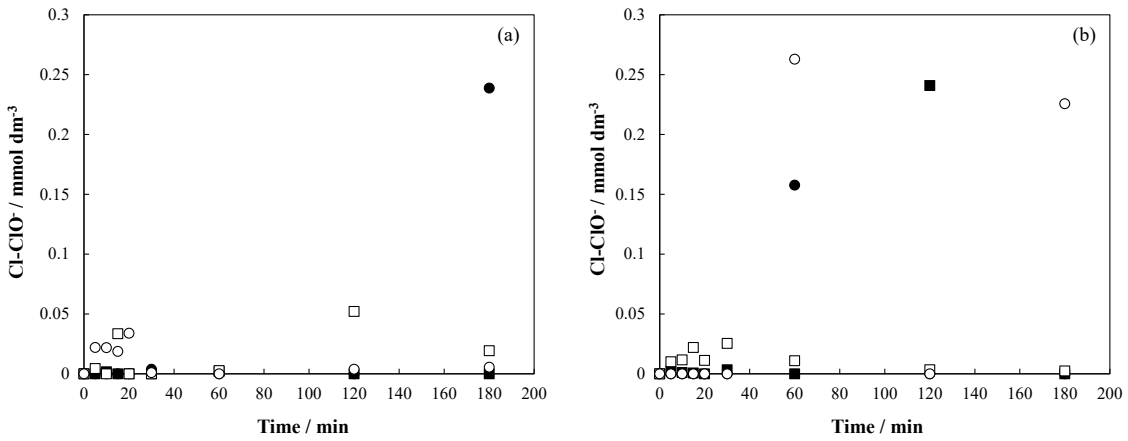

312 **Fig. 3.** Time course of the concentration of hypochlorite during the treatment of hospital
313 urines. Black symbols: electrolysis; white symbols: photoelectrolysis; (■, □) 5 A m^{-2}; (●,
314 ○) 50 A m^{-2}; (a) BDD anode; (b) MMO anode.

315 The amount of electrogenerated hypochlorite is lower than 0.3 mmol dm^{-3} Cl, regardless
316 the current density and the anode material used. However, it should be pointed out that
317 the hypochlorite measured is referred to the free concentration that has not reacted in the
318 effluent and much higher amounts are expected to have been generated during the
319 treatment. To check this hypothesis, electrolysis of 1000 mg dm^{-3} KCl was carried out
320 (Fig. S2a) since this compound is contained in the urine matrix in the same concentration.
321 In these tests, electrogenerated hypochlorite is expected to be easily accumulated because
322 it cannot react with other species as occur in the urine matrix. Results confirm that large
323 amounts of hypochlorite are generated at higher current densities (50 A m^{-2}).
324 Nevertheless, the concentration of this species is very low at 5 A m^{-2}, which implies that
325 higher values are required to ensure a significant production of hypochlorite during
326 electrolysis. This also supports the low disinfection rates registered during the treatment
327 of hospital urines under these conditions (5 A m^{-2}) where it is not possible to achieve 1
328 order of magnitude removal. Furthermore, it can be observed that the electrochemical
329 production of hypochlorite is influenced by the anode material used. Specifically,

concentrations around 1.8 mmol dm^{-3} Cl are achieved with MMO anodes at 50 A m^{-2} whereas the use of BDD anodes leads to the generation of concentrations lower than 0.6 mmol dm^{-3} Cl at the end of the process under the same operating conditions. This confirms the better electrocatalytic properties of the MMO anode tested to produce chlorine disinfectants and the subsequent removal of *K. pneumoniae* from urine.

Hypochlorite concentration does not follow a clear trend during the disinfection tests, and it could be related to the high reactivity of this species in the urine matrix: 1) hypochlorite can promote to other chlorine compounds in high oxidation state (i.e., chlorite, chlorate, and perchlorate) (Eqs. 5-7), 2) the photoactivation of hypochlorite can occur by the irradiation of UV light, favoring the production of free chlorine radicals (Eq. 8), 3) the degradation of organics naturally contained in urine (urea, creatinine and uric acid) can take place by chlorination reaction or 4) hypochlorite can react with ammonium contained in the effluent, favoring the production of combined chlorine species (chloramines) (Eqs. 9-11). All these reactions can occur simultaneously during the process.

$$ClO^- + H_2O \rightarrow ClO_2^- + 2\,H^+ + 2\,e^- \quad (E^0 = -1.67\ V) \tag{5}$$

$$ClO_2^- + H_2O \rightarrow ClO_3^- + 2\,H^+ + 2\,e^- \quad (E^0 = -1.18\ V) \tag{6}$$

$$ClO_3^- + H_2O \rightarrow ClO_4^- + 2\,H^+ + 2\,e^- \quad (E^0 = -1.20\ V) \tag{7}$$

$$ClO^- + h\nu \rightarrow Cl\cdot + O\cdot^- \quad (E^0 = 2.43\ V) \tag{8}$$

$$NH_4^+ + ClO^- \rightarrow NH_2Cl + H_2O \tag{9}$$

$$NH_2Cl + ClO^- \rightarrow NHCl_2 + H_2O \tag{10}$$

$$NHCl_2 + ClO^- \rightarrow NCl_3 + OH^- \tag{11}$$

351 The formation of chlorate and perchlorate was not detected by ion chromatography for
352 all the tests carried out with BDD and MMO anodes. The measured concentration was
353 below the detection limit for each species (ClO_3^-: 7 μg dm^{-3}; ClO_4^-: 7 μg dm^{-3}). This data
354 is of great importance because it reveals that the removal of ARB from urine by
355 electrolysis and photoelectrolysis could be carried out under the operating conditions
356 tested without the generation of undesirable chlorine by-products.
357 On the other hand, the concentration of free chlorine radicals is difficult to measure owing
358 to their short lifetime. Thus, to evaluate the possible formation of these species during the
359 disinfection of hospital urines by photoelectrolysis, experiments with 1000 mg dm^{-3} were
360 performed (Fig. S2b). As can be observed, the concentration of hypochlorite increases
361 with the operation time at 50 A m^{-2} whereas a negligible concentration was obtained at 5
362 A m^{-2} for both anodes. This behavior is similar to that previously obtained during single
363 electrolysis of KCl solutions (Fig. S2a). However, the concentration achieved is lower
364 during photoelectrolysis which indicates that hypochlorite has been photoactivated,
365 favoring the production of free chlorine radicals (Eq. 8). Therefore, the occurrence of
366 these radicals can be considered as one way for electrogenerated hypochlorite
367 consumption during photoelectrolysis of hospital urines.
368 Regarding the chlorination reaction of organics, urine contains large amounts of urea,
369 creatinine, and uric acid which are susceptible to react with hypochlorite during the
370 electrochemical treatment, decreasing their concentration [9]. The concentration of urea
371 remained constant for all the tests carried out with both anodes. Creatinine concentration
372 decreased between 10 and 25 % at 5 A m^{-2} and, up to 40 % at 50 A m^{-2} with BDD anodes
373 whereas its concentration remained constant when using MMO anodes, regardless the
374 current density applied. Finally, a percentage removal of uric acid around 50 % was
375 achieved during electrolysis and photoelectrolysis with BDD and MMO anodes at 5 and

376 50 A m^{-2} (data not shown). These reactions could promote the formation of
377 organochlorinated compounds in hospital urines which may increase the toxicity of the
378 resulting effluents. Nonetheless, their generation and accumulation are not expected to be
379 very high due to the low applied electric charges required for killing microorganisms. The
380 degradation of urea, creatinine and uric acid releases a higher nitrogen load to the effluent
381 which can be transformed into other inorganic species [59]. Specifically, nitrite is formed
382 from the oxidation of organic nitrogen released (Eq. 12, which is rapidly oxidized to
383 nitrate (Eqs. 13-14). Besides, this last species can be electrochemically reduced, favoring
384 the generation of ammonium (Eqs. 15-16) [60]. Hence, the concentration of ammonium
385 could be considered as an indirect measurement of the degradation of organics during the
386 disinfection of urines. Fig. 4 shows the time course of the ammonium concentration
387 during the disinfection of hospital urines by electrolysis and photoelectrolysis with BDD
388 and MMO anodes at different current densities. The initial amount in the urine matrix is
389 around 1.26 mmol dm^{-3} N.

390 $$N_{org} + O_{2(aq)} + e^- \rightarrow NO_2^- \quad (12)$$

391 $$3\ NO_2^- + 2\ H^+ \leftrightarrows 2\ NO_{(aq)} + NO_3^- + H_2O \quad (13)$$

392 $$NO_2^- + ½\ O_{2(aq)} \rightarrow NO_3^- \quad (14)$$

393 $$NO_3^- + 6\ H_2O + 8\ e^- \rightarrow NH_{3(aq)} + 9\ OH^- \quad (15)$$

394 $$NH_{3(aq)} + H_2O \rightleftharpoons NH_4^+ + OH^- \quad (16)$$

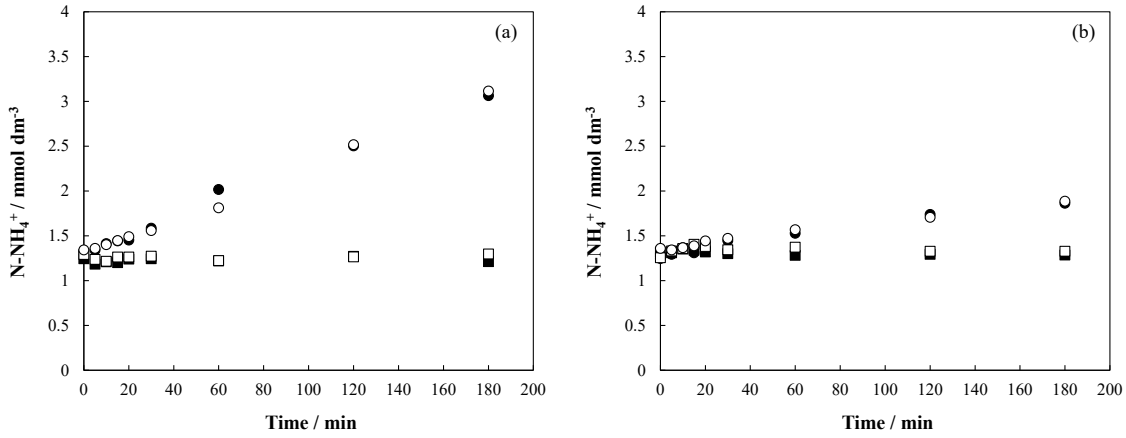

Fig. 4. Time course of the concentration of ammonium during the treatment of hospital urines. Black symbols: electrolysis; white symbols: photoelectrolysis; (■, □) 5 A m^{-2}; (●, ○) 50 A m^{-2}; (a) BDD anode; (b) MMO anode.

As can be observed, the concentration of ammonium remains constant at 5 A m^{-2} for both anodes. This suggests that the organics removal rate is very low, and the chlorination of organics does not lead to the release of nitro groups but the formation of organochlorinated compounds. Likewise, this low current density does not favor the production of other oxidants that could be generated and contribute to the removal of organics contained in urine. On the contrary, ammonium concentration continuously increases with the operation time at 50 A m^{-2}, being higher when working with BDD anodes. These results suggest that the electrogenerated hypochlorite could also be consumed in the degradation of organics contained in the urine matrix together with other oxidants generated during electrolysis and photoelectrolysis under these conditions. However, the irradiation of UV light does not influence the removal of organics since similar results are observed in both processes, regardless the anode material tested. The use of MMO anodes seems to be less effective for the removal of organics than BDD. This is an unexpected behavior considering the previous disinfection data where BDD anode showed lower rates for killing bacteria. At this point, it is important to remark that

414 the removal of organics can also take place by direct oxidation over the anode surface and
415 hydroxyl radical-mediated oxidation [36] and these mechanisms seem to be more relevant
416 when using BDD anodes at 50 A m^{-2}. Hence, there could be a marked competitive reaction
417 between the disinfection and the oxidation of organics with this anode.

418 Nonetheless, ammonium released could also be consumed together with the
419 electrogenerated hypochlorite to form chloramines (Eqs. 9-11) during the disinfection of
420 urines. This could explain the low concentration registered with MMO anodes since the
421 electrogeneration of hypochlorite is also expected to be higher with this anode (Fig. S2a).
422 For this reason, the concentration of chloramines was also monitored during the
423 disinfection of urines by electrolysis and photoelectrolysis and, the results obtained as
424 function of the operation time for both anodes at different current densities are plotted in
425 Fig. 5.

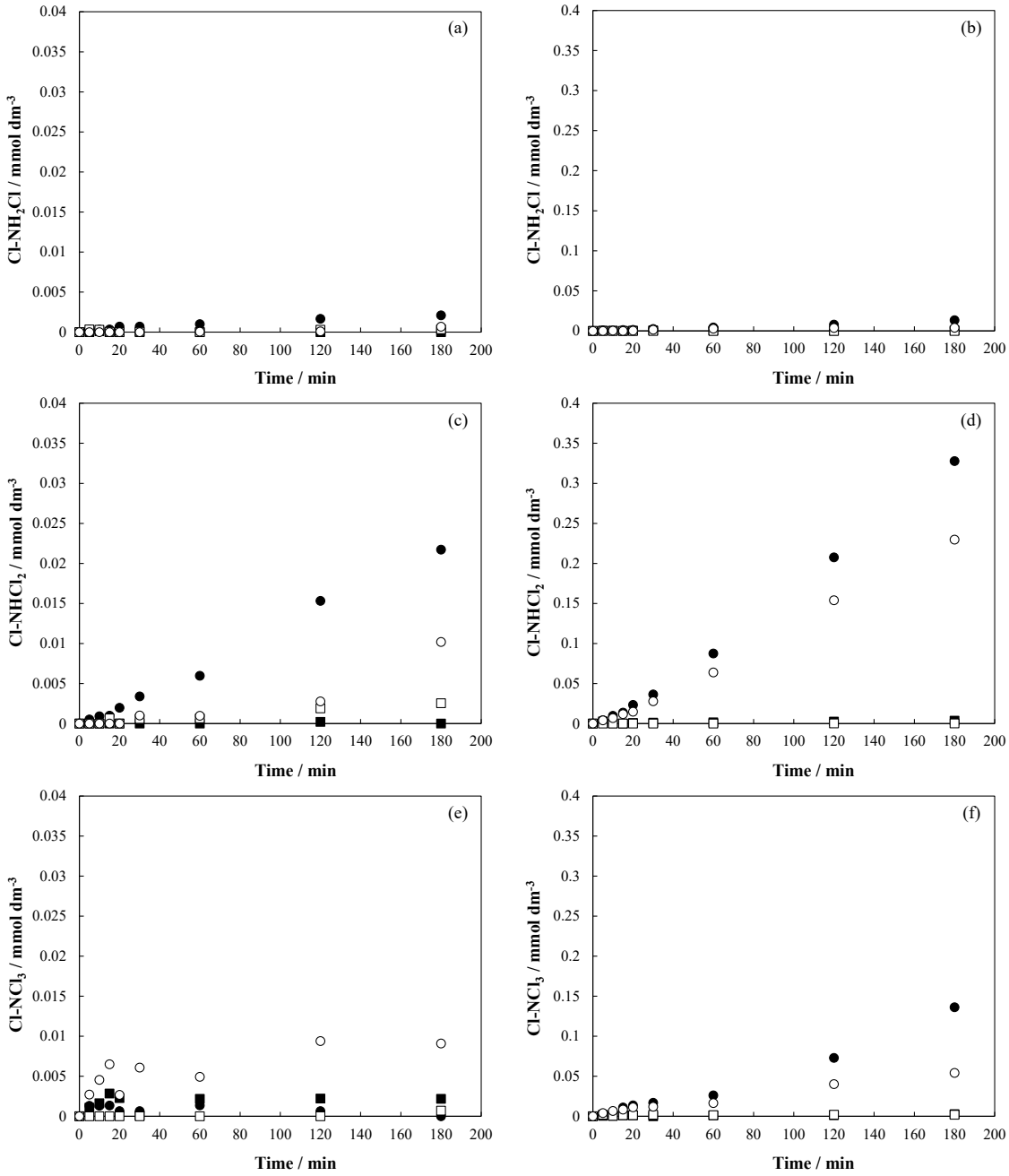

427 **Fig. 5.** Time course of the concentration of chloramines during the treatment of hospital
428 urines. Black symbols: electrolysis; white symbols: photoelectrolysis (■, □) 5 A m^{-2}; (●,
429 ○) 50 A m^{-2}; (a) Monochloramine-BDD; (b) Monochloramine-MMO; (c) Dichloramine-
430 BDD; (d) Dichloramine-MMO; (e) Trichloramine-BDD; (f) Trichloramine-MMO.

431 The concentration of chloramines increases with the operation time, being one order of
432 magnitude higher when using MMO anodes. This can be due to the large amounts of

433 hypochlorite generated with this anode and, it also seems to confirm that the formation of
434 chloramines is the main way of consumption of hypochlorite with MMO anodes whereas
435 the use of BDD anodes promotes the oxidation of organics. Chloramines also contribute
436 to the disinfection of urine although their disinfectant capacity is lower than hypochlorite.
437 Likewise, the presence of chloramines minimizes the production of trihalomethanes
438 (THMs) and trihalogenated haloacetic acids as disinfection by-products [61, 62] and,
439 hence, decreases the accumulation of hazardous organochlorinated compounds in treated
440 effluents. The formation of chloramines follows a sequential reaction that starts with the
441 generation of monochloramine (Eq. 9). This species is the most reactive chloramine and
442 it has been widely used for the disinfection of wastewater [63, 64]. Then,
443 monochloramine can be continuous to react with hypochlorite, favoring the formation of
444 dichloramine (Eq. 10), and, finally, trichloramine is formed by the reaction between
445 dichloramine and hypochlorite (Eq. 11). The presence of one or another chloramine will
446 depend mainly on the ratio Cl/N and the pH of the effluent [65]. In this context, hospital
447 urines used in this work present a pH value around 6, and, according to literature, it favors
448 the presence of dichloramine. This agrees with the results obtained during electrolysis
449 and photoelectrolysis at 50 A m^{-2} where dichloramine is the predominant species followed
450 by trichloramine and, finally, monochloramine. At low current densities, the
451 concentration of chloramines is negligible owing to the low concentration of hypochlorite
452 electrogenerated.

453 Overall, the concentration of chloramines is lower during photoelectrolysis and it can be
454 related to the photoactivation of hypochlorite (Eq. 8) that decreases its free concentration
455 to form chloramines. Likewise, the low concentration of monochloramine (Figs. 5a, 5b)
456 registered for both anodes can be explained by the photoactivation of this species (Eq.
457 17) [66]. In this context, monochloramine can be decomposed in free amine and chlorine

458 radicals by the irradiation of UV light. This also helps to remove ARB from urine since
459 chlorine radical significantly contributes to the disinfection process. The higher the
460 concentration of hypochlorite, the higher the concentration of chloramines and, hence,
461 the higher the concentration of free chlorine radicals during photoelectrolysis. This
462 supports the disinfection results from Fig. 1 because the concentration of hypochlorite is
463 expected to be higher with MMO anodes and the removal rates are also higher with this
464 anode.

465 $$NH_2Cl + h\nu \rightarrow NH_2\cdot + Cl\cdot \quad (17)$$

466 Finally, to evaluate the energy requirements of the combined process in comparison with
467 UV disinfection, the specific electric energy (E_{EO}) was calculated by Equations 18 and
468 19, where E_{cell} is the cell voltage (V), I the current intensity (kA), t the operation time (h),
469 V the volume (m^3), C_0 and C_f the initial and final bacteria concentration after 1 order of
470 magnitude removal (CFU ml^{-1}), respectively and W_{lamp} the power of the lamp used (kW).
471 This parameter determines the electric energy required to decrease the population of *K.*
472 *pneumoniae* by one order of magnitude in a unit volume [67]. The results obtained are
473 plotted in Fig. 6.

474 $$E_{EO} = \frac{E_{cell}\cdot I\cdot t}{V\cdot Log\frac{C_0}{C_f}} \quad (18)$$

475 $$E_{EO} = \frac{W_{lamp}\cdot t}{V\cdot Log\frac{C_0}{C_f}} \quad (19)$$

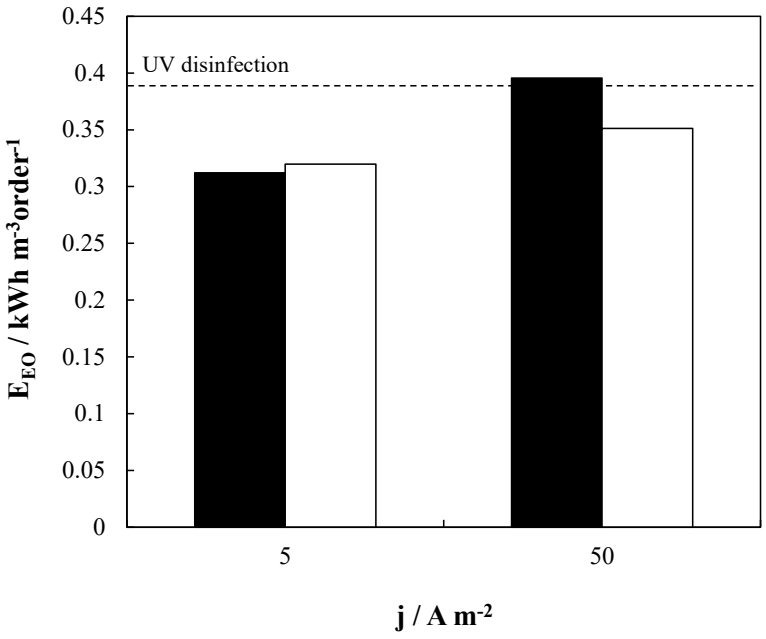

Fig. 6. Specific electric energy during UV disinfection and photoelectrolysis of hospital urines. Line: UV disinfection; black bars: BDD anode; white bars: MMO anode.

As can be observed, the lowest electric energy resulted in the combined process at low current densities using both BDD and MMO anodes. These results are in line with the synergistic effects found previously, where the highest values resulted when applying 5 A m^{-2}. At 50 A m^{-2}, the electric energy for the process with BDD anodes is slightly higher than that required for the UV disinfection process (0.395 *vs*. 0.389 kWh m^{-3} order^{-1}). Nevertheless, the use of MMO anodes at higher current densities leads to lower electric energy.

This reveals that electrolysis improves the efficiencies obtained during the UV disinfection process, decreasing, in turn, the energy requirements. This good performance of the combined process could be explained in terms of the promotion of free chlorine radicals. However, the use of BDD anodes is limited to their application at lower current densities, whereas MMO anodes can be used for all the current densities studied.

4. Conclusions

UV disinfection allows to decrease the population of ARB in synthetic hospital urine, but it cannot reach complete disinfection. The irradiation of UV light to urine polluted with *K. pneumoniae* could be limited by the occurrence of bacteria agglomeration or a resistant subpopulation. On the other hand, electrochemical oxidation with BDD and MMO anodes leads to complete removal of ARB from urine when applying 50 A m^{-2}. At 5 A m^{-2}, bacteria removal is negligible because the concentration of disinfectants produced is rather low. The disinfection rate is higher when working with MMO anodes and it can be related to competitive oxidation between bacteria and the organics contained in urine, which seems to be favored using BDD anodes. Finally, photoelectrolysis enhances single UV disinfection and electrolysis performances for all the current densities tested with BDD and MMO anodes. A more remarkable contribution of UV disinfection is observed at the beginning of the process whereas the electrochemical process has more influence at the end of the treatment. A marked synergistic effect was found when UV disinfection was enhanced by electrolysis at 5 A m^{-2} with BDD and MMO anodes. The use of BDD anodes at 50 A m^{-2} led to antagonistic effects due to the possible competitive degradation between bacteria and organics under these conditions. Regarding energy requirements for single and combined processes, the specific electric energy required for photoelectrolysis at low current densities is lower than that required for UV disinfection. At high current densities, MMO shows lower electric energy whereas the use of BDD anodes leads to a slightly higher value than UV disinfection.

Acknowledgments

Financial support from Junta de Comunidades de Castilla-La Mancha (JCCM), European Union (European Regional Development Fund), and Ministry of Science and Innovation through the projects SBPLY/17/180501/000396, PID2019-110904RB-I00, and the grant SBPLY/18/180501/000009 (Miguel Herraiz-Carboné) are gratefully acknowledged. The Spanish Ministry of Economy, Industry, and Competitiveness and the European Union is also gratefully acknowledged through the project EQC2018-004469-P. Dr. Salvador Cotillas wishes to express his gratitude to the Spanish Ministry of Science, Innovation, and Universities for the "Juan de la Cierva-Incorporación" post-doctoral grant (IJC2018-036241-I).

References

[1] S. Rodriguez-Mozaz, S. Chamorro, E. Marti, B. Huerta, M. Gros, A. Sànchez-Melsió, C.M. Borrego, D. Barceló, J.L. Balcázar, Occurrence of antibiotics and antibiotic resistance genes in hospital and urban wastewaters and their impact on the receiving river, Water Research, 69 (2015) 234-242.

[2] D. Hocquet, A. Muller, X. Bertrand, What happens in hospitals does not stay in hospitals: antibiotic-resistant bacteria in hospital wastewater systems, Journal of Hospital Infection, 93 (2016) 395-402.

[3] J. Lienert, M. Koller, J. Konrad, C.S. McArdell, N. Schuwirth, Multiple-Criteria Decision Analysis Reveals High Stakeholder Preference to Remove Pharmaceuticals from Hospital Wastewater, Environmental Science & Technology, 45 (2011) 3848-3857.

[4] D. Mao, S. Yu, M. Rysz, Y. Luo, F. Yang, F. Li, J. Hou, Q. Mu, P.J.J. Alvarez, Prevalence and proliferation of antibiotic resistance genes in two municipal wastewater treatment plants, Water Res., 85 (2015) 458-466.

[5] J. Rodríguez-Chueca, C. García-Cañibano, R.J. Lepistö, Á. Encinas, J. Pellinen, J. Marugán, Intensification of UV-C tertiary treatment: Disinfection and removal of micropollutants by sulfate radical based Advanced Oxidation Processes, J. Hazard. Mater., 372 (2019) 94-102.

[6] L. Proia, A. Adriana, S. Jessica, B. Carles, F. Marinella, L. Marta, B.J. Luis, P. Servais, Antibiotic resistance in urban and hospital wastewaters and their impact on a receiving freshwater ecosystem, Chemosphere, 206 (2018) 70-82.

[7] C. Bouki, D. Venieri, E. Diamadopoulos, Detection and fate of antibiotic resistant bacteria in wastewater treatment plants: A review, Ecotoxicology and Environmental Safety, 91 (2013) 1-9.

[8] S. Giannakis, B. Androulaki, C. Comninellis, C. Pulgarin, Wastewater and urine treatment by UVC-based advanced oxidation processes: Implications from the interactions of bacteria, viruses, and chemical contaminants, Chemical Engineering Journal, 343 (2018) 270-282.

[9] S. Cotillas, E. Lacasa, C. Sáez, P. Cañizares, M.A. Rodrigo, Disinfection of urine by conductive-diamond electrochemical oxidation, Appl. Catal. B Environ., 229 (2018) 63-70.

[10] J. Singla, V.K. Sangal, A. Singh, A. Verma, Application of mixed metal oxide anode for the electro-oxidation/disinfection of synthetic urine: Potential of harnessing molecular hydrogen generation, Journal of Environmental Management, 255 (2020) 109847.

[11] N. Gonzalez-Rivas, H. Reyes-Pérez, C.E. Barrera-Díaz, Recent Advances in Water and Wastewater Electrodisinfection, ChemElectroChem, 6 (2019) 1978-1983.

562 [12] E. Ortega-Gómez, M.M. Ballesteros Martín, B. Esteban García, J.A. Sánchez Pérez,
563 P. Fernández Ibáñez, Solar photo-Fenton for water disinfection: An investigation of the
564 competitive role of model organic matter for oxidative species, Applied Catalysis B:
565 Environmental, 148-149 (2014) 484-489.
566 [13] Y. Luo, L. Feng, Y. Liu, L. Zhang, Disinfection by-products formation and acute
567 toxicity variation of hospital wastewater under different disinfection processes,
568 Separation and Purification Technology, 238 (2020).
569 [14] B.R. Kim, J.E. Anderson, S.A. Mueller, W.A. Gaines, A.M. Kendall, Literature
570 review - Efficacy of various disinfectants against Legionella in water systems, Water
571 Res., 36 (2002) 4433-4444.
572 [15] J.R. Bolton, K.G. Linden, Standardization of methods for fluence (UV Dose)
573 determination in bench-scale UV experiments, J. Environ. Eng., 129 (2003) 209-215.
574 [16] C. Von Sonntag, Advanced oxidation processes: Mechanistic aspects, in: Water Sci.
575 Technol., 2008, pp. 1015-1021.
576 [17] W.A.M. Hijnen, E.F. Beerendonk, G.J. Medema, Inactivation credit of UV radiation
577 for viruses, bacteria and protozoan (oo)cysts in water: A review, Water Research, 40
578 (2006) 3-22.
579 [18] G. Wen, Q. Wan, X. Deng, R. Cao, X. Xu, Z. Chen, J. Wang, T. Huang, Reactivation
580 of fungal spores in water following UV disinfection: Effect of temperature, dark delay,
581 and real water matrices, Chemosphere, 237 (2019).
582 [19] E. Lacasa, S. Cotillas, C. Saez, J. Lobato, P. Cañizares, M.A. Rodrigo,
583 Environmental applications of electrochemical technology. What is needed to enable full-
584 scale applications?, Current Opinion in Electrochemistry, 16 (2019) 149-156.

585 [20] C.A. Martínez-Huitle, M.A. Rodrigo, I. Sirés, O. Scialdone, Single and Coupled
586 Electrochemical Processes and Reactors for the Abatement of Organic Water Pollutants:
587 A Critical Review, Chemical Reviews, 115 (2015) 13362-13407.
588 [21] A.S. Raut, G.B. Cunningham, C.B. Parker, E.J.D. Klem, B.R. Stoner, M.A.
589 Deshusses, J.T. Glass, Disinfection of E. coli contaminated urine using boron-doped
590 diamond electrodes, J Electrochem Soc, 161 (2014) G81-G85.
591 [22] A. Cano, C. Barrera, S. Cotillas, J. Llanos, P. Cañizares, M.A. Rodrigo, Use of
592 DiaCell modules for the electro-disinfection of secondary-treated wastewater with
593 diamond anodes, Chemical Engineering Journal, 306 (2016) 433-440.
594 [23] A. Kraft, M. Stadelmann, M. Blaschke, D. Kreysig, B. Sandt, F. Schröder, J. Rennau,
595 Electrochemical water disinfection. Part I: Hypochlorite production from very dilute
596 chloride solutions, Journal of Applied Electrochemistry, 29 (1999) 861-868.
597 [24] J. Jeong, C. Kim, J. Yoon, The effect of electrode material on the generation of
598 oxidants and microbial inactivation in the electrochemical disinfection processes, Water
599 Research, 43 (2009) 895-901.
600 [25] M.I. Kerwick, S.M. Reddy, A.H.L. Chamberlain, D.M. Holt, Electrochemical
601 disinfection, an environmentally acceptable method of drinking water disinfection?,
602 Electrochimica Acta, 50 (2005) 5270-5277.
603 [26] I. Sirés, E. Brillas, M.A. Oturan, M.A. Rodrigo, M. Panizza, Electrochemical
604 advanced oxidation processes: Today and tomorrow. A review, Environ. Sci. Pollut. Res.,
605 21 (2014) 8336-8367.
606 [27] C. Sáez, P. Cañizares, J. Llanos, M.A. Rodrigo, The Treatment of Actual Industrial
607 Wastewaters Using Electrochemical Techniques, Electrocatalysis, 4 (2013) 252-258.

608 [28] H. Bergmann, A discussion on diamond electrodes for water disinfection
609 electrolysis, Zur Bewertung von Diamantelektroden für die
610 Wasserdesinfektionselektrolyse, 151 (2010) 604-613.
611 [29] J. Isidro, D. Brackemeyer, C. Sáez, J. Llanos, J. Lobato, P. Cañizares, T. Matthée,
612 M.A. Rodrigo, Testing the use of cells equipped with solid polymer electrolytes for
613 electro-disinfection, Science of the Total Environment, 725 (2020).
614 [30] S. Giannakis, T.T.M. Le, J.M. Entenza, C. Pulgarin, Solar photo-Fenton disinfection
615 of 11 antibiotic-resistant bacteria (ARB) and elimination of representative AR genes.
616 Evidence that antibiotic resistance does not imply resistance to oxidative treatment, Water
617 Research, 143 (2018) 334-345.
618 [31] G.C. Lee, D.S. Burgess, Treatment of Klebsiella Pneumoniae Carbapenemase (KPC)
619 infections: A review of published case series and case reports, Ann. Clin. Microbiol.
620 Antimicrob., 11 (2012).
621 [32] G. Bitton, Wastewater microbiology, John Wiley & Sons, 2005.
622 [33] E.A. Serna-Galvis, E. Vélez-Peña, P. Osorio-Vargas, J.N. Jiménez, L. Salazar-
623 Ospina, Y.M. Guaca-González, R.A. Torres-Palma, Inactivation of carbapenem-resistant
624 Klebsiella pneumoniae by photo-Fenton: Residual effect, gene evolution and
625 modifications with citric acid and persulfate, Water Research, 161 (2019) 354-363.
626 [34] J.F. Pérez, J. Llanos, C. Sáez, C. López, P. Cañizares, M.A. Rodrigo, Development
627 of an innovative approach for low-impact wastewater treatment: A microfluidic flow-
628 through electrochemical reactor, Chemical Engineering Journal, 351 (2018) 766-772.
629 [35] S. Cotillas, D. Clematis, P. Cañizares, M.P. Carpanese, M.A. Rodrigo, M. Panizza,
630 Degradation of dye Procion Red MX-5B by electrolytic and electro-irradiated
631 technologies using diamond electrodes, Chemosphere, 199 (2018) 445-452.

632 [36] M. Panizza, G. Cerisola, Direct and mediated anodic oxidation of organic pollutants,
633 Chemical Reviews, 109 (2009) 6541-6569.
634 [37] S. Cotillas, E. Lacasa, C. Sáez, P. Cañizares, M.A. Rodrigo, Removal of
635 pharmaceuticals from the urine of polymedicated patients: A first approach, Chemical
636 Engineering Journal, 331 (2018) 606-614.
637 [38] J. Dupont, F. Dumont, C. Menanteau, M. Pommepuy, Calibration of the impedance
638 method for rapid quantitative estimation of Escherichia coli in live marine bivalve
639 molluscs, Journal of Applied Microbiology, 96 (2004) 894-902.
640 [39] S. Zhu, S. Schnell, M. Fischer, Rapid detection of Cronobacter spp. with a method
641 combining impedance technology and rRNA based lateral flow assay, Int. J. Food
642 Microbiol., 159 (2012) 54-58.
643 [40] A. WPCF, APHA, Standard Methods for the Examination of Water and Wastewater,
644 20th Ed, American Public Health Association (APHA), Washington DC, (1998).
645 [41] A.v. Wilpert, Über die Analyse von Hypochlorit und Chlorit in einer Lösung, Z.
646 Anal. Chem., 155 (1957) 378-378.
647 [42] H. Freytag, Zur Bestimmung von Hypochlorit, Chlorid und Chlorat in Chlorkalk, Z.
648 Anal. Chem., 171 (1959) 458-458.
649 [43] K. Oguma, H. Katayama, H. Mitani, S. Morita, T. Hirata, S. Ohgaki, Determination
650 of Pyrimidine Dimers in Escherichia coli and Cryptosporidium parvum during UV Light
651 Inactivation, Photoreactivation, and Dark Repair, APPL. ENVIRON. MICROBIOL., 67
652 (2001) 4630-4637.
653 [44] S. Vilhunen, H. Särkkä, M. Sillanpää, Ultraviolet light-emitting diodes in water
654 disinfection, Environ. Sci. Pollut. Res., 16 (2009) 439-442.

655 [45] M. Guo, H. Hu, J.R. Bolton, M.G. El-Din, Comparison of low- and medium-pressure
656 ultraviolet lamps: Photoreactivation of Escherichia coli and total coliforms in secondary
657 effluents of municipal wastewater treatment plants, Water Research, 43 (2009) 815-821.
658 [46] S. Cotillas, J. Llanos, M.A. Rodrigo, P. Cañizares, Use of carbon felt cathodes for
659 the electrochemical reclamation of urban treated wastewaters, Applied Catalysis B:
660 Environmental, 162 (2015) 252-259.
661 [47] C.D.N. Brito, D.M. De Araújo, C.A. Martínez-Huitle, M.A. Rodrigo, Understanding
662 active chlorine species production using boron doped diamond films with lower and
663 higher sp3/sp2 ratio, Electrochemistry Communications, 55 (2015) 34-38.
664 [48] P. Canizares, C. Sáez, F. Martínez, M.A. Rodrigo, The role of the characteristics of
665 p-Si BDD anodes on the efficiency of wastewater electro-oxidation processes,
666 Electrochemical and Solid-State Letters, 11 (2008) E15-E19.
667 [49] J.P. De Paiva Barreto, K.C. De Freitas Aráujo, D.M. De Aráujo, C.A. Martínez-
668 Huitle, Effect of sp3/sp2 ratio on boron doped diamond films for producing persulfate,
669 ECS Electrochemistry Letters, 4 (2015) E9-E11.
670 [50] I. Moraleda, S. Cotillas, J. Llanos, C. Sáez, P. Cañizares, L. Pupunat, M.A. Rodrigo,
671 Can the substrate of the diamond anodes influence on the performance of the
672 electrosynthesis of oxidants?, Journal of Electroanalytical Chemistry, 850 (2019) 113416.
673 [51] W. Feng, A. Deletic, Z. Wang, X. Zhang, T. Gengenbach, D.T. McCarthy,
674 Electrochemical oxidation disinfects urban stormwater: Major disinfection mechanisms
675 and longevity tests, Science of The Total Environment, 646 (2019) 1440-1447.
676 [52] A. Sánchez-Carretero, C. Sáez, P. Cañizares, M.A. Rodrigo, Electrochemical
677 production of perchlorates using conductive diamond electrolyses, Chemical Engineering
678 Journal, 166 (2011) 710-714.

679 [53] S. Cotillas, M.J.M. de Vidales, J. Llanos, C. Sáez, P. Cañizares, M.A. Rodrigo,
680 Electrolytic and electro-irradiated processes with diamond anodes for the oxidation of
681 persistent pollutants and disinfection of urban treated wastewater, Journal of Hazardous
682 Materials, 319 (2016) 93-101.
683 [54] F.L. Souza, C. Sáez, P. Cañizares, M.A. Rodrigo, Improving photolytic treatments
684 with electrochemical technology, Separation and Purification Technology, 235 (2020).
685 [55] M. Herraiz-Carboné, S. Cotillas, E. Lacasa, P. Cañizares, M.A. Rodrigo, C. Sáez,
686 Removal of antibiotic resistant bacteria by electrolysis with diamond anodes: A
687 pretreatment or a tertiary treatment?, J. Water Process Eng., 38 (2020) 101557.
688 [56] D. Golub, E. Ben-Hur, Y. Oren, A. Soffer, Electroadsorption of bacteria on porous
689 carbon and graphite electrodes, Bioelectrochemistry and Bioenergetics, 17 (1987) 175-
690 182.
691 [57] S. Cotillas, J. Llanos, P. Cañizares, S. Mateo, M.A. Rodrigo, Optimization of an
692 integrated electrodisinfection/electrocoagulation process with Al bipolar electrodes for
693 urban wastewater reclamation, Water Research, 47 (2013) 1741-1750.
694 [58] D. Ghernaout, B. Ghernaout, From chemical disinfection to electrodisinfection: The
695 obligatory itinerary?, Desalination and Water Treatment, 16 (2010) 156-175.
696 [59] M.J. Martin De Vidales, M. Millán, C. Sáez, P. Cañizares, M.A. Rodrigo, What
697 happens to inorganic nitrogen species during conductive diamond electrochemical
698 oxidation of real wastewater?, Electrochemistry Communications, 67 (2016) 65-68.
699 [60] E. Lacasa, P. Cañizares, J. Llanos, M.A. Rodrigo, Effect of the cathode material on
700 the removal of nitrates by electrolysis in non-chloride media, Journal of Hazardous
701 Materials, 213-214 (2012) 478-484.

[61] F. Wang, B. Gao, D. Ma, R. Li, S. Sun, Q. Yue, Y. Wang, Q. Li, Effects of operating conditions on trihalomethanes formation and speciation during chloramination in reclaimed water, Environ. Sci. Pollut. Res., 23 (2016) 1576-1583.

[62] A.C. Diehl, G.E. Speitel Jr., J.M. Symons, S.W. Krasner, C.J. Hwang, S.E. Barrett, DBP formation during chloramination, Journal AWWA, 92 (2000) 76-90.

[63] K. Doederer, W. Gernjak, H.S. Weinberg, M.J. Farré, Factors affecting the formation of disinfection by-products during chlorination and chloramination of secondary effluent for the production of high quality recycled water, Water Research, 48 (2014) 218-228.

[64] J. Le Roux, M.J. Plewa, E.D. Wagner, M. Nihemaiti, A. Dad, J.P. Croué, Chloramination of wastewater effluent: Toxicity and formation of disinfection byproducts, J. Environ. Sci., 58 (2017) 135-145.

[65] A.T. Palin, The determination of free chlorine and of chloramine in water using p-aminodimethylaniline, Analyst, 70 (1945) 203-207.

[66] B. Jiang, Y. Tian, Z. Zhang, Z. Yin, L. Feng, Y. Liu, L. Zhang, Degradation behaviors of Isopropylphenazone and Aminopyrine and their genetic toxicity variations during UV/chloramine treatment, Water Research, 170 (2020) 115339.

[67] J.R. Bolton, K.G. Bircher, W. Tumas, C.A. Tolman, Figures-of-merit for the technical development and application of advanced oxidation technologies for both electric- and solar-driven systems (IUPAC Technical Report), 73 (2001) 627.

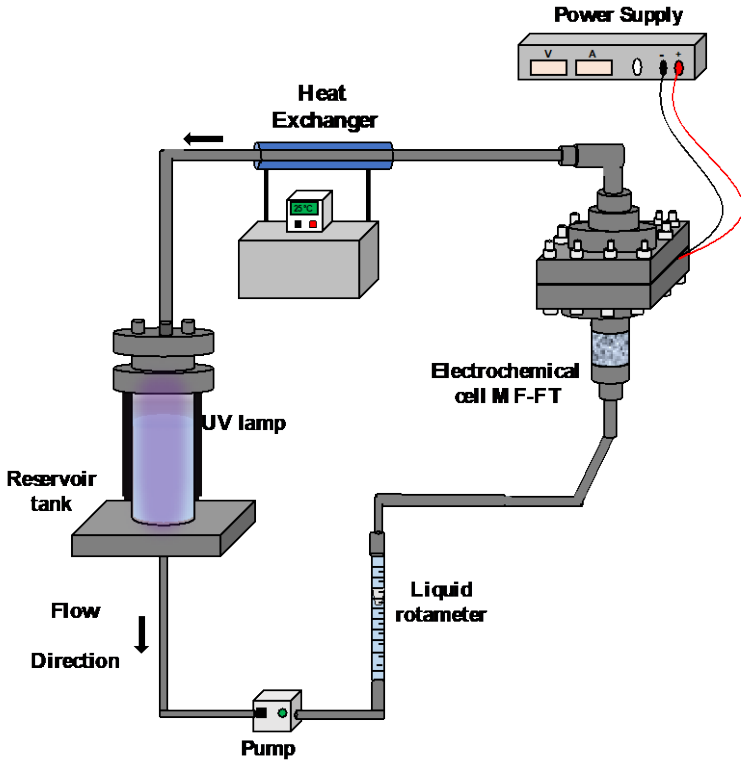

727 **Fig. S1.** Experimental setup.

728

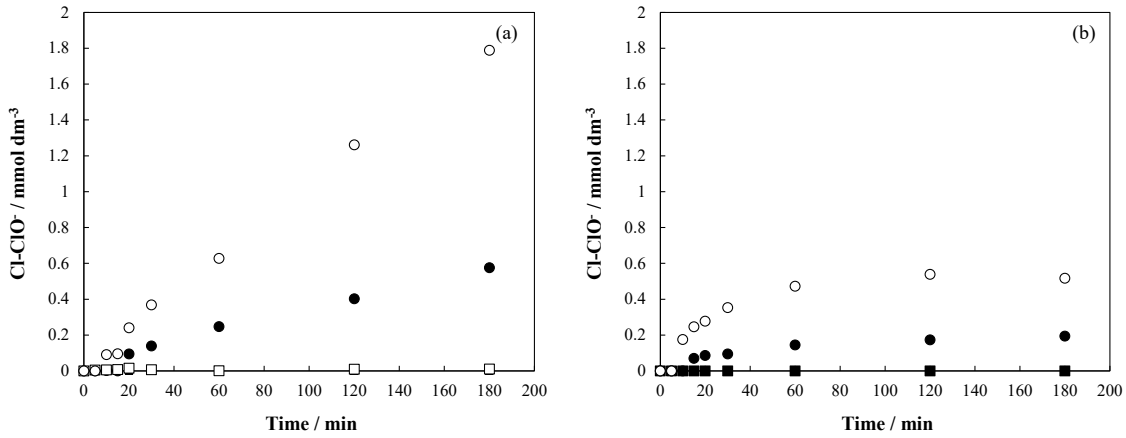

730 **Fig. S2.** Time course of the concentration of hypochlorite during the electrolysis of 1000
731 mg dm^{-3} KCl. Black symbols: BDD anode; white symbols: MMO anode; (■, □) 5 A m^{-2};
732 (●, ○) 50 A m^{-2}; (a) electrolysis; (b) photoelectrolysis.

733